Improving liver fibrosis diagnosis based on forward and backward second harmonic generation signals

Citation: Peng, Qiwen et al. "Improving Liver Fibrosis Diagnosis Based on Forward and Backward Second Harmonic Generation Signals." Applied Physics Letters 106, 8 (February 2015): 083701 © 2015 AIP Publishing LLC

As Published: http://dx.doi.org/10.1063/1.4913907

Publisher: American Institute of Physics (AIP)

Persistent URL: http://hdl.handle.net/1721.1/119881

Version: Final published version: final published article, as it appeared in a journal, conference proceedings, or other formally published context

Improving liver fibrosis diagnosis based on forward and backward second harmonic generation signals

Qiwen Peng,[1,2,3,4] Shuangmu Zhuo,[1,2,a)] Peter T. C. So,[1,3,5,6] and Hanry Yu[1,3,4,6,7,8,a)]
[1]*Biosystems and Micromechanics IRG, Singapore-MIT Alliance for Research and Technology, 1 CREATE Way, #04-13/14 Enterprise Wing, Singapore 138602*
[2]*Institute of Laser and Optoelectronics Technology, Fujian Normal University, Fuzhou 350007, China*
[3]*Computation and System Biology Program, Singapore-MIT Alliance, 4 Engineering Drive 3, E4-04-10, Singapore 117576*
[4]*Institute of Bioengineering and Nanotechnology, A*STAR, The Nanos, 31 Biopolis Way, #04-01, Singapore 138669*
[5]*Department of Mechanical Engineering, Massachusetts Institute of Technology, Cambridge, Massachusetts 02139, USA*
[6]*Department of Biological Engineering, Massachusetts Institute of Technology, Cambridge, Massachusetts 02139, USA*
[7]*Department of Physiology, Yong Loo Lin School of Medicine, National University of Singapore, Singapore, Singapore 117597*
[8]*Mechanobiology Institute, National University of Singapore, Singapore, Singapore 117411*

(Received 10 December 2014; accepted 19 February 2015; published online 26 February 2015)

The correlation of forward second harmonic generation (SHG) signal and backward SHG signal in different liver fibrosis stages was investigated. We found that three features, including the collagen percentage for forward SHG, the collagen percentage for backward SHG, and the average intensity ratio of two kinds of SHG signals, can quantitatively stage liver fibrosis in thioacetamide-induced rat model. We demonstrated that the combination of all three features by using a support vector machine classification algorithm can provide a more accurate prediction than each feature alone in fibrosis diagnosis. © *2015 AIP Publishing LLC*. [http://dx.doi.org/10.1063/1.4913907]

Liver fibrosis is the consequence of a sustained wound-healing response to chronic hepatocellular damage and it may result in cirrhosis, liver failure, and portal hypertension.[1] Collagen accumulation is one of the most significant phenomena and diagnostic characteristics in liver fibrosis development.

Due to its noncentrosymmetric structure, collagen is able to produce a second harmonic generation (SHG) signal, which is intrinsic and requires no fluorophore presence in tissue. Therefore, SHG microscopy has been used for collagen quantification as an indicator of fibrosis progression,[2–6] especially in liver.[7–9] However, most studies only focused on the use of forward SHG signal to diagnosis liver fibrosis.

Recently, it has been recognized that forward and backward SHG signals are generated simultaneously, and different morphological features of collagen fibrils were extracted in forward SHG and backward SHG images.[10] For example, researchers studied and confirmed that the ratio of forward SHG to backward SHG signals arises from fibril size and packing. This concept has been used to differentiate healthy and diseased tissues in osteogenesis imperfect (OI),[11] ovarian cancer,[12] and breast cancer.[13] Therefore, the combination of forward SHG and backward SHG signals may provide in tandem complementary information about collagen and provide a useful means to improve liver fibrosis diagnosis.

The primary goal of this work is to investigate the feasibility of using the combination of forward SHG and backward SHG signals for improving liver fibrosis diagnosis in a well-established disease model.[14] In this study, we not only validated feasibility of differentiating between normal and fibrotic liver tissues from forward SHG, backward SHG, and their average intensity ratio but also quantitatively monitored the evolution of collagen through the whole liver fibrosis progression by comparing with morphological staging performed by pathologists, which is considered to be the existing gold standard for liver fibrosis diagnosis.[15,16] Furthermore, a support vector machine (SVM) algorithm was performed to effectively improve the diagnostic accuracy at different fibrosis stages based on the combination of all extracted features.

A total of 40 male Wistar rats at an average weight of 220 g were used to establish the liver fibrosis model. Thioacetamide (TAA) was administrated into the rats through intra-periotoneal injection (i.p.) with 200 mg/kg of body weight with Phosphate Buffer Solution (PBS), three times a week for 14 weeks. Rats were sacrificed at week 0 (control), 2, 4, 6, 8, 10, 12, and 14 after liver fibrosis induction ($n = 5$ per week). After cardiac perfusion with 4% paraformaldehyde to flush out blood cells and fix the tissue, livers were extracted, paraffinized, and sectioned with a thickness of 5 μm and 50 μm for staining and SHG imaging, respectively. Tissue samples of 5 μm were stained with a Masson Trichrome (MT) stain kit (Chroma View advanced testing, No. 87019, Richard-Allan Scientific, Thermo Fisher Scientific, Wathan, Massachusetts) and classified into stage 0, 1, 2, 3, and 4 by a pathologist based on blind reading to reduce any bias using Metavir score.[17] Tissue samples of 50 μm from 5 rats in each scored stage were used for SHG imaging. The nonlinear optical system was developed based on a confocal imaging system (LSM 510, Carl Zeiss,

a)Authors to whom correspondence should be addressed. Electronic addresses: shuangmuzhuo@gmail.com and hanry_yu@nuhs.edu.sg

Heidelberg, Germany) as described in our previous work.[18,19] The excitation light comes from a femtosecond mode-lock Ti:saphire laser (Mai-Tai broadband, Spectra-Physics) tuned to 900 nm, passing through a pulse compressor (Femtocontrol, APE GmbH, Berlin, Germany) and an acousto-optic modulator (AOM) for group velocity dispersion compensation and power attenuation, respectively. An oil immersion objective of numerical aperture of 1.3 (Calr Zeiss: EC Plan-Neofluar, 40×) was used for microscopic imaging. The beam focuses on specimen after being reflected by a dichroic mirror (KP 650) that deflects laser light longer than 650 nm and allows transmission of light shorter than 650 nm. Forward SHG was collected by a condenser (NA = 0.55) and filtered by a 450 ± 10 nm bandpass filter before entering photomultiplier tube (PMT). Backward SHG signal simultaneously generated in tissue was collected by the same objective lens and recorded by a spectral detector that includes 32-spectral channels and allows spectral detection between 430 and 750 nm. Emission beam at 450 ± 10 nm was recorded. Settings for both channels were kept the same for all images through the whole experiment. In each scored stage, 20 images per sample were acquired and each one has $225 \times 225\ \mu m^2$ field of view with 1024 × 1024 pixels. A fine focusing stage (HRZ 200 stage, Carl Zeiss) was used to change and record the focus position and to translate the samples after x-y scan of the samples. The depth of 0 μm refers to the tissue surface where the signal of reflection from the interface between the tissue and the glass coverslip reaches to maximum.

Morphology of collagen fibers at different pathological fibrosis stages were visualized by the nonlinear optical system from both forward and backward aspects of SHG signals. The previous studies have demonstrated that the intensity ratio of the forward and backward signals increases with increasing depth.[11,20] Therefore, considering the variation with depth, the same focal plane at the depth of 2 μm was analyzed for each sample. Fig. 1 shows selected images that reflect typical characteristics of collagen accumulation in the tissue with the development of liver fibrosis. Both forward and backward SHG signals are able to present fine collagen fibers in high resolution. In early stages (control and stage 1), collagen mainly locates around portal tracts and central veins as thin circles. More and more collagen is generated at both around vessel area and tissue in later stages. Collagen around vessels gets thicker and extends until it links with collagen from other vessels, forming broad septa between portal areas and between portal areas and central veins. This phenomenon is a key criterion for late stage fibrosis assessment in various score systems.[21–25] Therefore, it is obvious that clear changes of collagen deposition during fibrotic progression can be recorded by both forward SHG and backward SHG images from nonlinear optical approach without any staining.

Quantification is required for diagnostic purpose, especially for fibrosis staging. To accurately extract collagen information from SHG images, Gaussian mixture model based segmentation method is utilized. This method was shown to be more accurate than other methods such as global thresholding and clustering methods.[26] After segmentation, final masks were created on both raw forward SHG and backward SHG images to present collagen content in the tissue

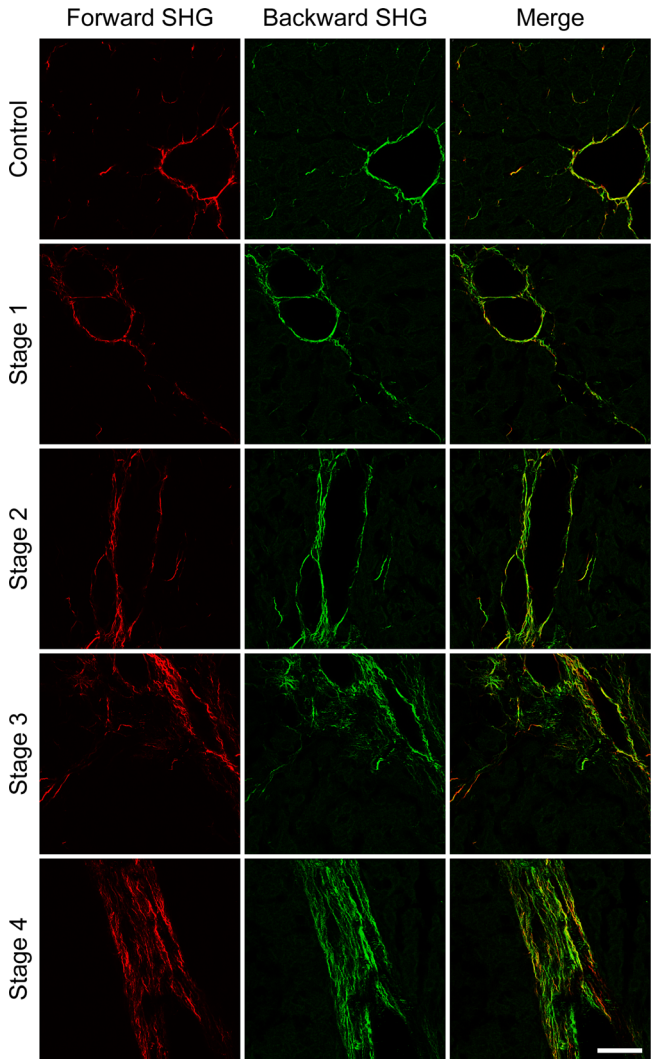

FIG. 1. Forward SHG and backward SHG signals from collagen at different liver fibrosis stages. Both forward SHG signals (first column, false color as red) and backward SHG signals (second column, false color as green) show significantly increment of collagen deposition with the development of fibrosis from control (first row) to late stages (rows 2–5 correspond to stages 1–4, respectively). Merged images (third column) indicate the perfect overlay of forward and backward SHG signals. Scale bar is 50 μm.

samples. The segmentation results of forward SHG, backward SHG, and the overlap area are shown in Fig. 2(A). From the segmentation images, collagen area percentage can be calculated through dividing the number of pixels that belongs to collagen by total area of an image. Fig. 2(B) indicates that total collagen area percentage increases significantly with the natural progression of liver fibrosis and evidently reflects different stages based on histo-pathological results. The quantitative result shows capability of both forward SHG and backward SHG of collagen for liver fibrosis staging and this is in good agreement with the previous experiments.

Nevertheless, collagen fibrils in forward and backward SHG images are not completely colocalized even though their final collagen area percentages are at highly similar levels for all stages. The difference is due to the coherent nature of SHG that it has a phase (and spatial) relationship with the laser excitation. This characteristic underlies the observed contrast in the forward and backward modes and provides a

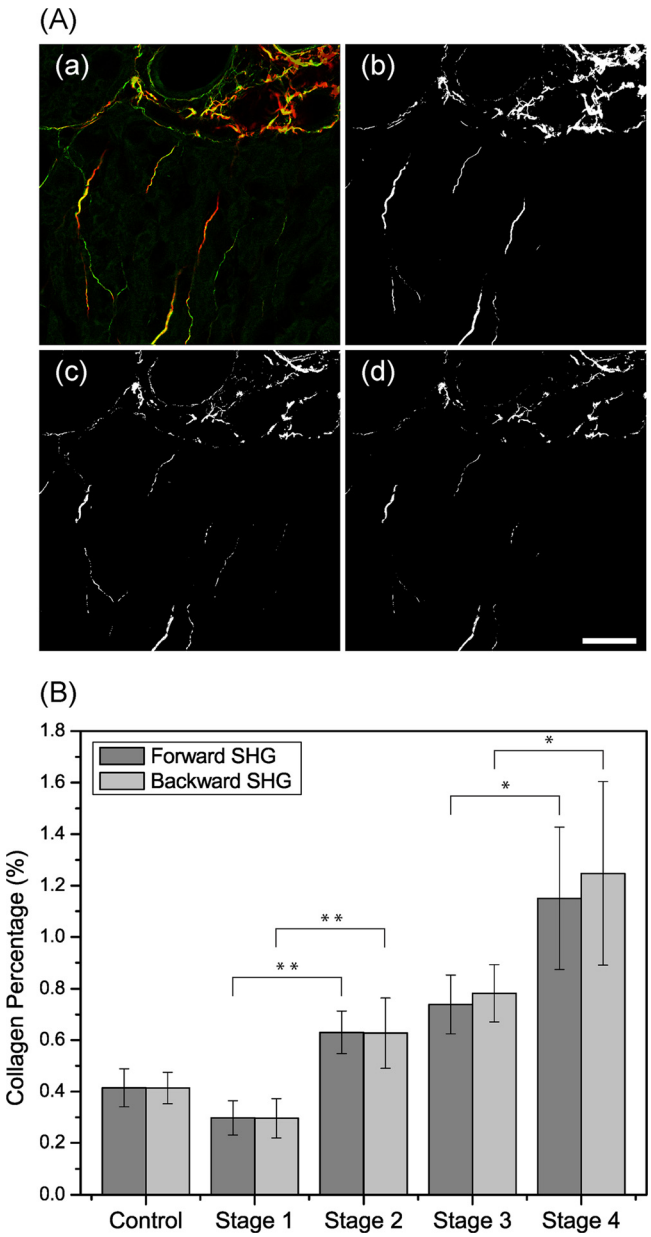

FIG. 2. Quantification of liver fibrosis progression from areas of collagen detected by nonlinear microscopy. (A) Segmentation results of both forward SHG (b) and backward SHG (c) images using Gaussian mix model based algorithm are able to preserve collagen distribution and morphology. Even though the signals from two channels are highly colocalized (a), a certain area is not exactly overlapped (d). Scale bar is 50 μm. (B) Collagen area percentage quantified from forward SHG and backward SHG images, respectively, and they are significantly increased with the fibrosis progression. Comparison between two adjacent stages is performed with student's t-test. Significant differences ($*p < 0.05$, $**p < 0.01$) exist between stage 1 vs. stage 2 and stage 3 vs. stage 4. There are no significant differences between normal vs. stage 1 and stage 2 vs. stage 3 ($p > 0.05$). Error bars represent standard deviation (SD).

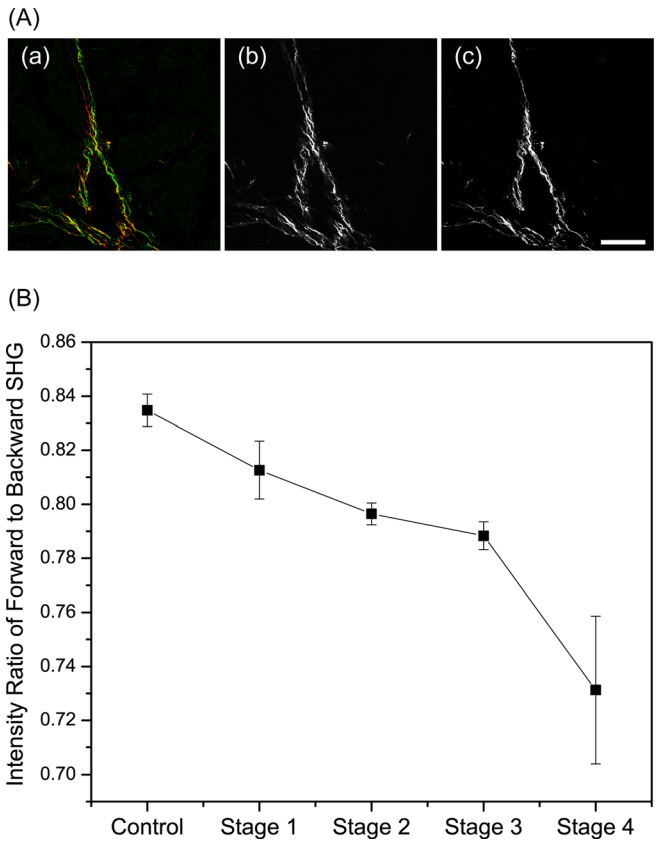

FIG. 3. Quantification of average intensity ratio of forward SHG to backward SHG signals. (A) Gray scaled forward SHG image (b) and backward SHG image (c) from original image (a). Scale bar is 50 μm. (B) Quantitative results from gray scaled images on average intensity ratio of forward SHG to backward SHG signals at different fibrosis stages. Error bars represent SD.

great more information about the structure of the collagen fibrils. Combining these two kinds of signals would possibly reveal the evolution of fibrillar collagen during fibrosis progression and further contribute to liver fibrosis diagnosis. Thus, the signal intensity ratios of forward SHG to backward SHG at different stages were studied as well. All images were grey scaled and saturated pixels were removed (Fig. 3(A)). Average intensities of all the rest of the pixels within collagen masks were calculated. Fig. 3(B) shows the ratio of average intensity of forward SHG to backward SHG acquired in same location. It illustrates that the intensity ratio decreases with the development of fibrotic status. The decrement can be adequately explained that a greater portion of collagen in late stages form septa which results in more backward light scattering, while less forward light is collected accordingly. Unlike the general results in the literature, the forward SHG signal is smaller than backward SHG signal. Three main factors, we believe, contribute to this result. First, as the chosen focal plane is close to the surface of tissue (2 μm), there will be a higher probability of multiple scatterings along the direction of forward SHG instead of the direction of backward SHG. Therefore, the ratio of forward SHG to backward SHG will be less than 1 and subsequently increases if we focus deeper into the specimen.[11,20] Second, the objective lens for backward SHG detection and the condenser for forward SHG detection have different NA. The collection angle of forward channel is smaller than that of backward channel. Third, the signal attenuations of forward and backward SHG are different due to different optical paths.

Although the above three quantitative assessments (forward SHG collagen area percentage, backward SHG collagen area percentage, average intensity ratio of forward SHG to backward SHG) are able to identify different fibrosis stages base on histo-pathological scores, they describe the event from different aspects and are limited to be an reliable index for

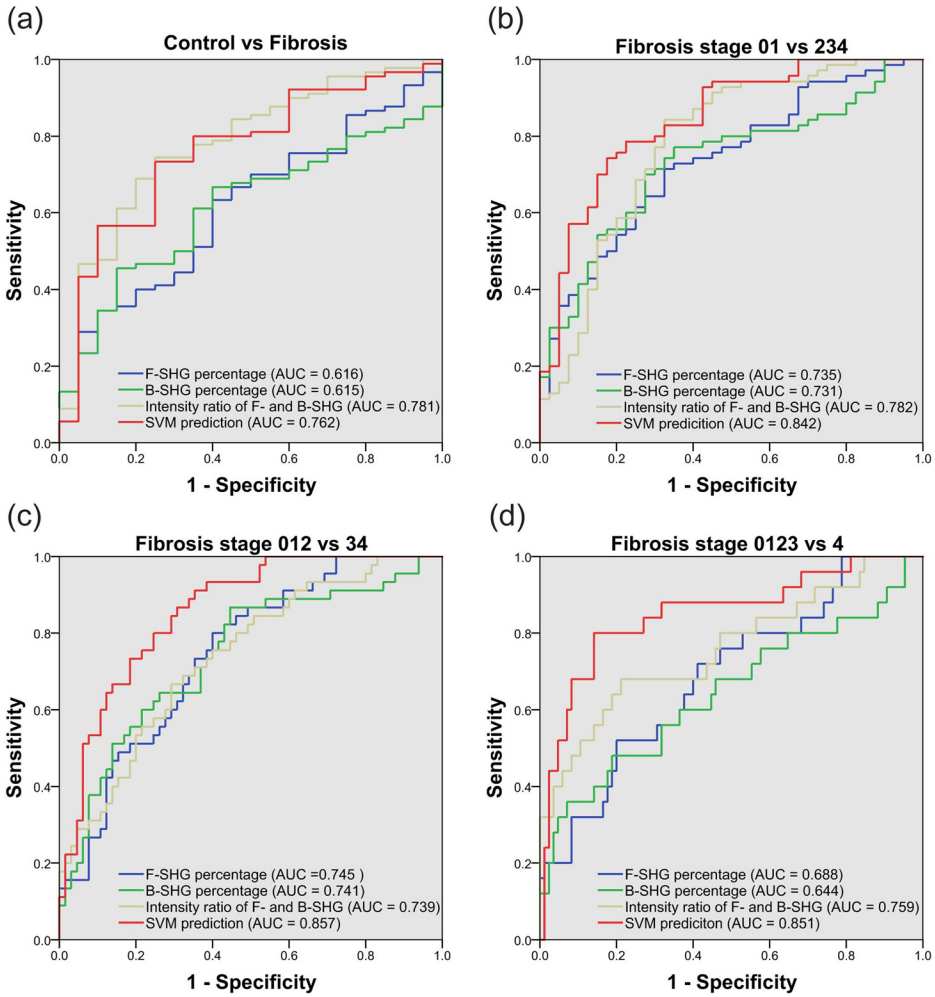

FIG. 4. Comparison of fibrosis staging differentiation ability by ROC curves of collagen area percentage from forward SHG signals (blue), collagen area percentage from backward SHG signals (green), average intensity ratio of forward SHG to backward SHG signals (brown), and SVM algorithm to combine the above three features (red).

liver fibrosis diagnosis alone. It is expected that the combination of all these features would provide more complementary information and improve the accuracy of the diagnosis. Therefore, a SVM classification method was chosen due to its advantage of classifying data measured from multiple signal sources (multivariate data) with relatively small sample sizes.[27] SVMs are supervised learning models in machine learning to analyze data with the purpose of separating them into different groups with a clear and widest gap. In this process, all data are set as points distributed in space. Even though SVMs are good at performing both linear and nonlinear classifications, they are especially competent in nonlinear ones which are suitable for multiple inputs. In this case, we used a pre-computed nonlinear SVM algorithm that is a radial basis function Kernel in LIBSVM (V3.17)[28] to classify the samples based on all the above three quantitative features. 10-fold cross-validation was utilized so that all samples were used for both training and validation to enhance the prediction accuracy. Receiver operating characteristic (ROC) curves of collagen percentage in forward SHG (blue), in backward SHG (green), intensity ratio of forward SHG to backward SHG (brown), and SVM classification results (red) were drawn according to different fibrosis stages (Fig. 4). It is clear that SVM results show a better prediction on fibrosis staging, especially in late stages. It means the combination of three features by SVM classification algorithm significantly improved fibrosis diagnosis compared to quantification of each feature alone. Specifically, the area under ROC curve (AUC) values of SVM results are 0.762, 0.842, 0.857, and 0.851 for distinguishing each adjacent stage, respectively.

In summary, the present paper validated the feasibility of a useful quantitative method by combining forward SHG and backward SHG signals from collagen for liver fibrosis staging. This method integrated three quantitative assessments, including the collagen content percentage of forward SHG, the collagen content percentage of backward SHG, and the average intensity ratio of forward SHG to backward SHG signals. The combined results showed a more significant classification capability that would enhance accuracy of liver fibrosis diagnosis in each stage. Since the three features are acquired in one-time scanning, further imaging and more processing procedures are not required. So, this method renders a promising tool for diagnosis of liver fibrosis development in different stages more accurately.

This project was supported by the National Research Foundation Singapore, through the Singapore MIT Alliance for Research and Technology (SMART) Centre's BioSyM IRG research programme. This project also was supported in part by the Institute of Bioengineering and Nanotechnology, Biomedical Research Council, A*STAR; grants from Janssen (R-185-000-182-592 and R-185-000-228-592), Singapore-MIT Alliance Computational and Systems Biology Flagship Project funding (C-382-641-001-091), and SMART BioSyM

and Mechanobiology Institute of Singapore (R-714-001-003-271). S.Z. thanks the National Key Basic Research Program of China (2015CB352006), the National Natural Science Foundation of China (61275006 and 61335011), the Fujian Provincial Youth Top-notch Talent Support Program, the Natural Science Foundation for Distinguished Young Scholars of Fujian Province (2014J06016), the Program from Education Bureau of Fujian Province (JA12057 and JA13060), and the Program for Changjiang Scholars and Innovative Research Team in University (Grant No. IRT1115) for financial support.

[1]R. Bataller and D. A. Brenner, J. Clin. Invest. **115**(2), 209 (2005).
[2]X. Han, R. M. Burke, M. L. Zettel, P. Tang, and E. B. Brown, Opt. Express **16**(3), 1846 (2008).
[3]T. A. Theodossiou, C. Thrasivoulou, C. Ekwobi, and D. L. Becker, Biophys. J. **91**(12), 4665 (2006).
[4]B. Gong, J. Sun, G. Vargas, Q. Chang, Y. Xu, D. Srivastava, and P. J. Boor, Birth Defects Res., Part A **82**(1), 16 (2008).
[5]C. Odin, Y. Le Grand, A. Renault, L. Gailhouste, and G. Baffet, J. Microsc. **229**(Pt. 1), 32 (2008).
[6]M. Strupler, A. M. Pena, M. Hernest, P. L. Tharaux, J. L. Martin, E. Beaurepaire, and M. C. Schanne-Klein, Opt. Express **15**(7), 4054 (2007).
[7]W. Sun, S. Chang, D. C. Tai, N. Tan, G. Xiao, H. Tang, and H. Yu, J. Biomed. Opt. **13**(6), 064010 (2008).
[8]M. D. Gorrell, X. M. Wang, M. T. Levy, E. Kable, G. Marinos, G. Cox, and G. W. McCaughan, Adv. Exp. Med. Biol. **524**, 235 (2003).
[9]G. Cox, E. Kable, A. Jones, I. Fraser, F. Manconi, and M. D. Gorrell, J. Struct. Biol. **141**(1), 53 (2003).
[10]M. Suzuki, D. Kayra, W. M. Elliott, J. C. Hogg, and T. Abraham, Proc. SPIE **8226**, 82263F (2012).
[11]R. Lacomb, O. Nadiarnykh, and P. J. Campagnola, Biophys. J. **94**(11), 4504 (2008).
[12]O. Nadiarnykh, R. B. LaComb, M. A. Brewer, and P. J. Campagnola, BMC Cancer **10**, 94 (2010).
[13]V. Ajeti, O. Nadiarnykh, S. M. Ponik, P. J. Keely, K. W. Eliceiri, and P. J. Campagnola, Biomed. Opt. Express **2**(8), 2307 (2011).
[14]M. Mitsuhashi, K. Morimura, H. Wanibuchi, A. Kiyota, S. Wada, T. Nakatani, and S. Fukushima, J. Toxicol. Pathol. **17**(3), 219 (2004).
[15]M. J. Ruwart, K. F. Wilkinson, B. D. Rush, T. J. Vidmar, K. M. Peters, K. S. Henley, H. D. Appelman, K. Y. Kim, D. Schuppan, and E. G. Hahn, Hepatology **10**(5), 801 (1989).
[16]D. Tretheway, A. Jain, R. LaPoint, R. Sharma, M. Orloff, P. Milot, A. Bozorgzadeh, and C. Ryan, Liver Transpl. **14**(5), 695 (2008).
[17]P. Bedossa and T. Poynard, Hepatology **24**(2), 289 (1996).
[18]D. C. Tai, N. Tan, S. Xu, C. H. Kang, S. M. Chia, C. L. Cheng, A. Wee, C. L. Wei, A. M. Raja, G. Xiao, S. Chang, J. C. Rajapakse, P. T. So, H. H. Tang, C. S. Chen, and H. Yu, J. Biomed. Opt. **14**(4), 044013 (2009).
[19]Y. He, C. H. Kang, S. Xu, X. Tuo, S. Trasti, D. C. Tai, A. M. Raja, Q. Peng, P. T. So, J. C. Rajapakse, R. Welsch, and H. Yu, J. Biomed. Opt. **15**(5), 056007 (2010).
[20]G. Hall, K. W. Eliceiri, and P. J. Campagnola, J. Biomed. Opt. **18**(11), 116008 (2013).
[21]K. P. Batts and J. Ludwig, Am. J. Surg. Pathol. **19**(12), 1409 (1995).
[22]V. J. Desmet, M. Gerber, J. H. Hoofnagle, M. Manns, and P. J. Scheuer, Hepatology **19**(6), 1513 (1994).
[23]K. Ishak, A. Baptista, L. Bianchi, F. Callea, J. De Groote, F. Gudat, H. Denk, V. Desmet, G. Korb, R. N. MacSween *et al.*, J. Hepatol. **22**(6), 696 (1995).
[24]R. G. Knodell, K. G. Ishak, W. C. Black, T. S. Chen, R. Craig, N. Kaplowitz, T. W. Kiernan, and J. Wollman, Hepatology **1**(5), 431 (1981).
[25]P. J. Scheuer, J. Hepatol. **13**(3), 372 (1991).
[26]S. Xu, D. C. Tai, P. T. So, H. Yu, and J. Rajapakse, Aust. J. Intell. Inf. Process. Syst. **12**(2), 146 (2010).
[27]C. Cortes and V. Vapnik, Mach. Learn. **20**(3), 273 (1995).
[28]C. Chang and C. Lin, LIBSVM, version 3.17, see www.csie.ntu.edu.tw/~cjlin/libsvm/.